Nano Research
2023, 16(4): 5247–5255

ISSN 1998-0124 CN 11-5974/O4
https://doi.org/10.1007/s12274-022-5153-1

Research Article

Enhancing bioactivity and stability of polymer-based material-tissue interface through coupling multiscale interfacial interactions with atomic-thin TiO_2 nanosheets

Rongchen Xu[1,2,§], Xiaodan Mu[1,§], Zunhan Hu[3,§], Chongzhi Jia[1], Zhenyu Yang[4], Zhongliang Yang[1], Yiping Fan[1], Xiaoyu Wang[1,5], Yuefeng Wu[6], Xiaotong Lu[6], Jihua Chen[4] (✉), Guolei Xiang[6] (✉), and Hongbo Li[1] (✉)

[1] *Department of Stomatology, The First Medical Center, Chinese PLA General Hospital, Beijing 100853, China*
[2] *Department of Stomatology, The Third Medical Center, Chinese PLA General Hospital, Beijing 100039, China*
[3] *Department of Stomatology, Kunming Medical University, Kunming 650500, China*
[4] *National Clinical Research Center for Oral Diseases & Shaanxi Key Laboratory of Stomatology, Department of Prosthodontics, School of Stomatology, The Fourth Military Medical University, Xi'an 710032, China*
[5] *Department of Stomatology, The Strategic Support Force Medical Center, Beijing 100101, China*
[6] *State Key Laboratory of Chemical Resource Engineering, College of Chemistry, Beijing University of Chemical Technology, Beijing 100029, China*
[§] *Rongchen Xu, Xiaodan Mu, and Zunhan Hu contributed equally to this work.*

Received: 9 August 2022 / **Revised:** 30 September 2022 / **Accepted:** 3 October 2022

ABSTRACT

Stable and bioactive material–tissue interface (MTF) basically determines the clinical applications of biomaterials in wound healing, sustained drug release, and tissue engineering. Although many inorganic nanomaterials have been widely explored to enhance the stability and bioactivity of polymer-based biomaterials, most are still restricted by their stability and biocompatibility. Here we demonstrate the enhanced bioactivity and stability of polymer-matrix bio-composite through coupling multiscale material–tissue interfacial interactions with atomically thin TiO_2 nanosheets. Resin modified with TiO_2 nanosheets displays improved mechanical properties, hydrophilicity, and stability. Also, we confirm that this resin can effectively stimulate the adhesion, proliferation, and differentiation into osteogenic and odontogenic lineages of human dental pulp stem cells using *in vitro* cell–resin interface model. TiO_2 nanosheets can also enhance the interaction between demineralized dentinal collagen and resin. Our results suggest an approach to effectively up-regulate the stability and bioactivity of MTFs by designing biocompatible materials at the sub-nanoscale.

KEYWORDS

material–tissue interface, TiO_2 nanosheets, pulpo-dentinal complex, biomaterial, resin composite

1 Introduction

Inorganic nanomaterials have been widely explored as structural reinforcements and functional components in bio-medical polymer-matrix composites (PMCs) for wound healing, sustained drug release, tissue engineering scaffold, etc. [1–4]. Such PMCs can protect tissues against mechanical forces (e.g., bite force, blood pressure, and friction) [5–8] and biochemical stimulations (e.g., bacterial, enzyme, and virus) [9–11], reduce infection risks and tissue degradation [12, 13], and provide mechanical supports [12–14]. Material–tissue interfaces (MTFs) between exogenous materials and bio-components (such as protein, collagen, and cell) can critically provide delivering channels for biological factors [15], protect collagen fibrils against degradation [16], and stimulate cellular responses like adhesion, proliferation and differentiation [17]. In general, material–tissue interactions (MTI) involve two scales of interfaces, atomic-level organic–inorganic interfaces in PMCs and microscale interfaces between PMCs and cells/tissues. Manipulating the physiochemical properties and bio-functions of PMCs can basically optimize the properties of such multiscale interfaces to enhance MTIs.

Interfacial adhesion is the primary property affecting the stability, physicochemical properties, biocompatibility, and bio-function of biomedical materials [18, 19]. This interfacial property can be generally enhanced through increasing the strength and density of interfacial bonds [20], which can be further controlled through varying the sizes and surface areas of filler particles, surface modification, physical treatments, and introducing coupling agents [21–23]. For biomedical PMCs, size and dimension of nanomaterials can critically affect interfacial adhesion and physiochemical performances [24]. For example, inspired by the liner ordered microstructures of bone, one-dimensional (1D) nanostructures such as hydroxyapatite (HAP) nano fibers have been widely explored in bone tissue engineering [25, 26]. Over last decade, two-dimensional (2D) nanomaterials, such as graphene, black phosphorous, and layered double hydroxides (LDHs), have also been explored as a new type of reinforcements for biomedical PMCs, because their large specific

Address correspondence to Jihua Chen, jhchen@fmmu.edu.cn; Guolei Xiang, xianggl@mail.buct.edu.cn; Hongbo Li, hongbo_l@sina.com

surface areas can provide more bonding sites with organic matrix and tissues [27–29]. Moreover, their high surface reactivity can strongly graft functional groups to interact with specific target and perform specific biofunctions like antibiosis, anti-virus, and stimulate cell responses. However, the practical medical applications of most materials are still limited by their surface bonding activity, stability, and biotoxicity. Therefore, exploring biocompatible 2D nanomaterials with enhanced interfacial adhesion and bioactivity is still on demand for developing promising biomedical materials.

TiO_2 nanostructures have been explored as promising fillers to improve the mechanical strength and biological activity of PMCs owing to high chemical inertness and biocompatibility, and inexpensive costs [30–32]. However, their applications are still limited by stability in PMCs. Herein we demonstrate the enhanced performances of TiO_2 nanosheets (TiO_2 NSs) to PMCs in cell-nanomaterial and collagen-nanomaterial interfacial interactions by human pulpo-dentinal complex. The complexity and diversity of oral microbiota, the masticatory force, and the anatomical structure of pulpo-dentinal complex make the dentin–resin interface as a challenging system to explore the effects of MTI, and we find that TiO_2 NSs can improve the hydrophilicity and mechanical properties of adhesive resin (AR) and form stable hybrid resin matrix surface. Adhesive resin composites (ARCs) modified with such TiO_2 NSs can promote the adhesion, proliferation, and osteogenic and odontogenic differentiation capacity of human dental pulp stem cells (hDPSCs) from pulp. Furthermore, TiO_2 NSs also improve the bonding stability between exogenous adhesive resin composites and human demineralized dentin collagen, leading to more stable material-collagen hybrid layers (Fig. 1(a).

2 Experimental section

TiO_2 NSs were prepared following a solvothermal method [33–35]. Then the TiO_2-ARCs were prepared through mechanical agitation for 10 min and ultrasonic blending for 10 min. Table 1 presents detailed formula. Degree of conversion (DC), elastic module, hardness, stability, hydrophilicity, and roughness of resin were evaluated. Then, intact non-caries human third molars were extracted and collected from the donors after signing informed consent to extract hDPSCs and be prepared as the dental bonding model. The protocol was approved by the Institutional Review Board of the last author's institute (#IRB-S2021-655-01). After isolation and identification of hDPSCs, the effect of TiO_2-ARCs on cell adhesion, proliferation, and differentiation was evaluated using cell counting kit-8 (CCK-8), scanning electron microscopy (SEM) observation, staining, quantitative real-time polymerase chain reaction (RT-qPCR), and Western blot analysis (WB). Furthermore, the interaction stability between demineralized dentin collagen and TiO_2-ARCs was tested through the interface strength test, fracture mode analysis, interface observation, and nano-leakage. Detail procedure of all tests and the statistic strategies are listed in the Electronic Supplementary Material (ESM).

3 Results and discussion

3.1 Preparation of TiO_2 NSs and TiO_2-ARCs

TiO_2 NSs were prepared following a solvothermal method by hydrolyzing $TiCl_4$ in ethylene glycol (EG), in which EG acts as both solvent and capping ligand. Transmission electron microscopy (TEM) image shows soft 2D nanosheet structure (Fig. 1(b)). X-ray diffraction (XRD) pattern can be indexed to monoclinic TiO_2(B) (PDF card 74-1940, Fig. 1(c)). These results indicate high purities in both morphology and phase of the TiO_2 NS.

TiO_2-ARCs were prepared with TiO_2 nanostructures and adhesive resin matrix. The resin matrix phase composes of commonly used resins in dentistry [36], including bisphenol-A glycol dimethacrylate (Bis-GMA) and hydroxyethyl methylacrylate (HEMA) (Fig. 1(d)). Camphorquinone (CQ) and ethyl 4-(di-methylamino) benzoate (EDMAB) were used as photoinitiation reagents. Resin matrixes without TiO_2 and filled with TiO_2 nanoparticles (NPs) were used as blank and positive control groups. All the adhesive resins can transform from liquid to solid under ultraviolet (UV) irradiation (Fig. 1(e)), yielding organic–inorganic surfaces. The pure resin is transparent, while the composites modified with TiO_2 nanostructures are opaque. TEM image shows that TiO_2 NSs were well dispersed in the composites (Fig. 1(f) and Fig. S1 in the ESM).

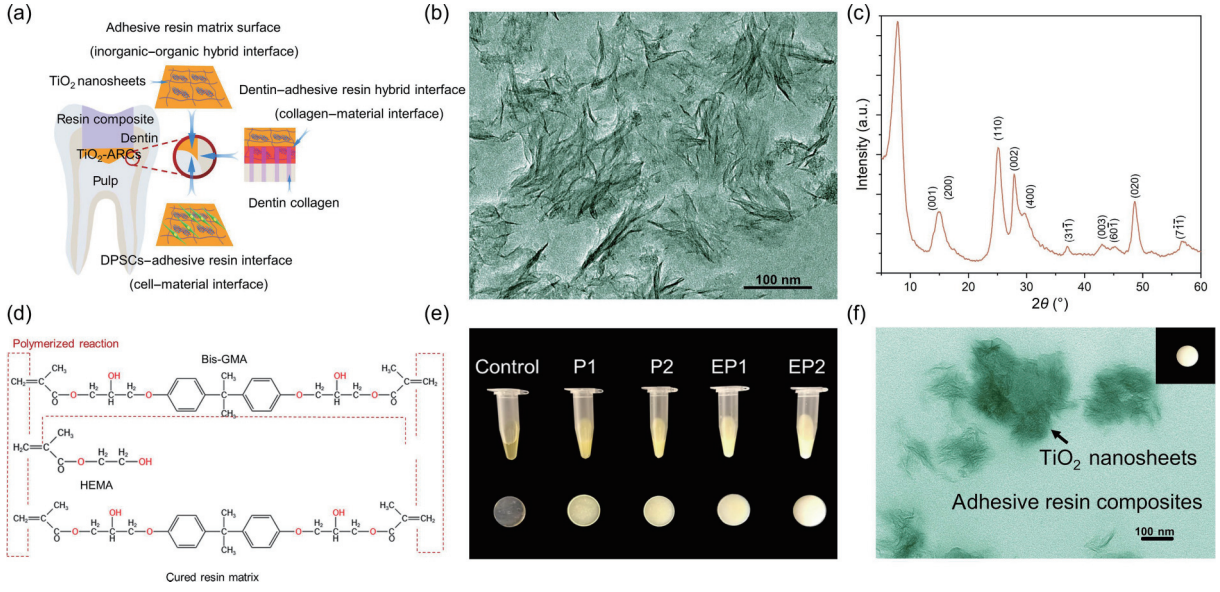

Figure 1 Composition and structure of TiO_2-ARCs. (a) Schematic diagram showing the multiscale interfaces in dental adhesive with TiO_2-ARCs. (b) TEM image and (c) XRD pattern of atomically thin TiO_2 NSs. (d) Monomers of adhesive resin composites. (e) ARCs images of different groups before and after polymerization. (f) TEM image showing the dispersion of TiO_2 NSs in ARCs.

Table 1 The formula of each tested adhesive resin composites

Groups	Formula of each group (g)					
	Bis-GMA	HEMA	CQ	EDMAB	TiO_2 NPs	TiO_2 NSs
Ctrl	6.6	3.3	0.05	0.05	—	—
P1	6.6	3.3	0.05	0.05	0.025	—
P2	6.6	3.3	0.05	0.05	0.05	—
EP1	6.6	3.3	0.05	0.05	—	0.025
EP2	6.6	3.3	0.05	0.05	—	0.05

3.2 Physicochemical properties of TiO_2-ARCs

We first studied the modification effects of TiO_2 NSs on the physicochemical properties of ARCs, which could basically regulate the stability and bioactivity of MTFs [37, 38]. The properties include DC, surface elastic module, hardness, thermal stability, water solubility (WSL), water sorption (WSp), surface wettability, and roughness [39–43].

DC represents liquid–solid phase transformation capacity of resin matrix [23], which is measured through attenuated total reflection-Fourier transform infrared (ATR-FTIR) spectrum. The values of all groups increase with light-curing time, and become stable within 80 s (Fig. 2(a) and Table S1 in the ESM). Addition of TiO_2 nanomaterials can lower DC values, which is inversely proportional to TiO_2 amounts. After light-curing for 80 s, experimental group 2 (EP2) shows the lowest DC value of 53.06 ± 0.52 (%) ($p < 0.05$). This trend results from the light-blocking effect of TiO_2, because TiO_2 can absorb and scatter UV lights in ARCs. TiO_2 NSs can more effectively reduce DC than TiO_2 NPs, suggesting TiO_2 NSs can more strongly inhibit polymerization. The higher specific surface area and reactivity of NSs may be the primary cause of this phenomenon. Polymerization of resin matrix is induced from the chain-growth reaction. After illumination, the free radicals of resin matrix are activated, then the electron transition and the rate of molecular bombardment are promoted, triggering chain reaction.

The addition of TiO_2 nanomaterials can enhance the mechanical strength of adhesive resin matrixes. At the same concentration, resin surface modified with TiO_2 NSs shows higher elastic module and hardness compared to TiO_2 NPs counterparts (Figs. 2(b) and 2(c), and Fig. S2 in the ESM). EP2 with 0.5 wt.% TiO_2 NSs shows the highest elastic module of 5.99 ± 0.29 GPa and hardness of 0.33 ± 0.02 GPa. TiO_2 NSs fillers insert into resin matrix molecular chains and compress their spaces, thus inhibiting their motions. Furthermore, the interactions between TiO_2 NSs and resin matrix molecules construct lock nodes, forming synergetic crosslinking interactions across multiscale interfaces, which can further enhance mechanical properties [44]. The interaction between TiO_2 NSs fillers and resin matrix molecular further leads to improved thermostability and lower solubility of the composites. Differential scanning calorimetry (DSC) curves show increased peak temperatures rise with the amounts of TiO_2 NSs. EP2 shows the highest peak temperature at 557.2 °C and the lowest WSL (Figs. 2(d) and 2(e)).

TiO_2 NSs can increase the hydrophilicity of resin surfaces, which is critical for bioactivity. The addition of TiO_2 nanostructures can increase water sorption rates and decrease contact angles of H_2O. The WSp of EP2 is significantly higher than others ($p < 0.05$) (Fig. 2(f)). The contact angles are 80.44° ± 0.46° for control group (Ctrl), 61.98° ± 1.36° for group 1 (P1), 57.60° ± 0.74° for group 2 (P2), 56.72° ± 0.68° for experimental group 1 (EP1), and 51.78° ± 0.76° for EP2 (Fig. 2(g) and Table S2 in the ESM). This is because TiO_2 nanostructures can increase the attraction interactions with H_2O through chemisorption and physisorption [45]. In particular, the larger surface area of TiO_2 NSs can provide more interaction sites with water molecules to improve hydrophilicity. In addition, roughness can also regulate surface hydrophobicity [45, 46]. We find that all groups do not show significant differences in surface roughness (Fig. 2(h) and Fig. S3 in the ESM), thus TiO_2 nanomaterials do not effectively modify the homogeneity of resin matrixes. Therefore, the increased hydrophilicity mainly results from the interaction of TiO_2 with H_2O rather than roughness.

3.3 Regulation capacity of cell-resin interface to cell bio-behaviors

Resin matrix has been widely applied in dentistry and orthopedics as adhesive, pulp capping, and scaffold reagents [46–49]. We use the adhesive resin matrixes as stem cell niche to investigate the regulatory capacity of TiO_2 NSs on cell bioactivity. Considering the potential clinical applications, hDPSCs were extracted from non-caries intact human teeth and cultured on targeted resin surfaces under proliferative conditions. Primary and continuous cells with fibroblast-like morphology were observed under optical microscope (Figs. 3(a) and 3(b)). NF-H staining (Fig. 3(c)) and Oil Red O staining (Fig. 3(d)) results demonstrated that the cultured cells have potential for neurogenic and adipogenic differentiations. The positive expression of stromal cell antigen 1 (STRO-1) suggested that the cultured cells have stemness (Fig. 3(e)). Therefore, the isolated cells are hDPSCs with multi-differentiation potential.

3.3.1 Cell adhesion and proliferation

Cell adhesion and proliferation are significant for regulating cell fates like differentiation and apoptosis [50, 51]. We use CCK-8, cytoskeleton staining, SEM, and immunofluorescence staining to evaluate regulation effects of physicochemical and mechanical properties of substrate surfaces on cell adhesion and proliferation *in vitro*. CCK-8 results show that TiO_2 NSs can significantly improve hDPSCs proliferation on resin matrix surfaces (Fig. 3(f)), also illustrate that the TiO_2-ARCs exhibit biocompatibility. The ratios of living cells in all groups increase with incubation time. Figure 3(g) shows the F-actin of hDPSCs in EP2 was more organized and extended than that in other groups. These extended actin fibers suggest that targeted hDPSCs can exert traction force on the substrates, which can increase adhesion strength. Figure 3(h) shows hDPSCs cultured on TiO_2-ARCs of EP2 exhibit more spreading pseudopods than other groups to provide more binding sites with exogenous substrates. This further verifies the introduction of TiO_2 NSs can significantly promote the hDPSCs adhesion.

Living-cell staining further verifies the up-regulation capacity of TiO_2 NSs on hDPSCs proliferation and shows that all cells display the typical long-spindle morphology (Fig. 3(i)). The amount of cells adhered on EP2 is about two times of that on P2, suggesting that TiO_2 NSs can more effectively improve cell activity than TiO_2 NPs. Cells adhere onto material surfaces through the interaction

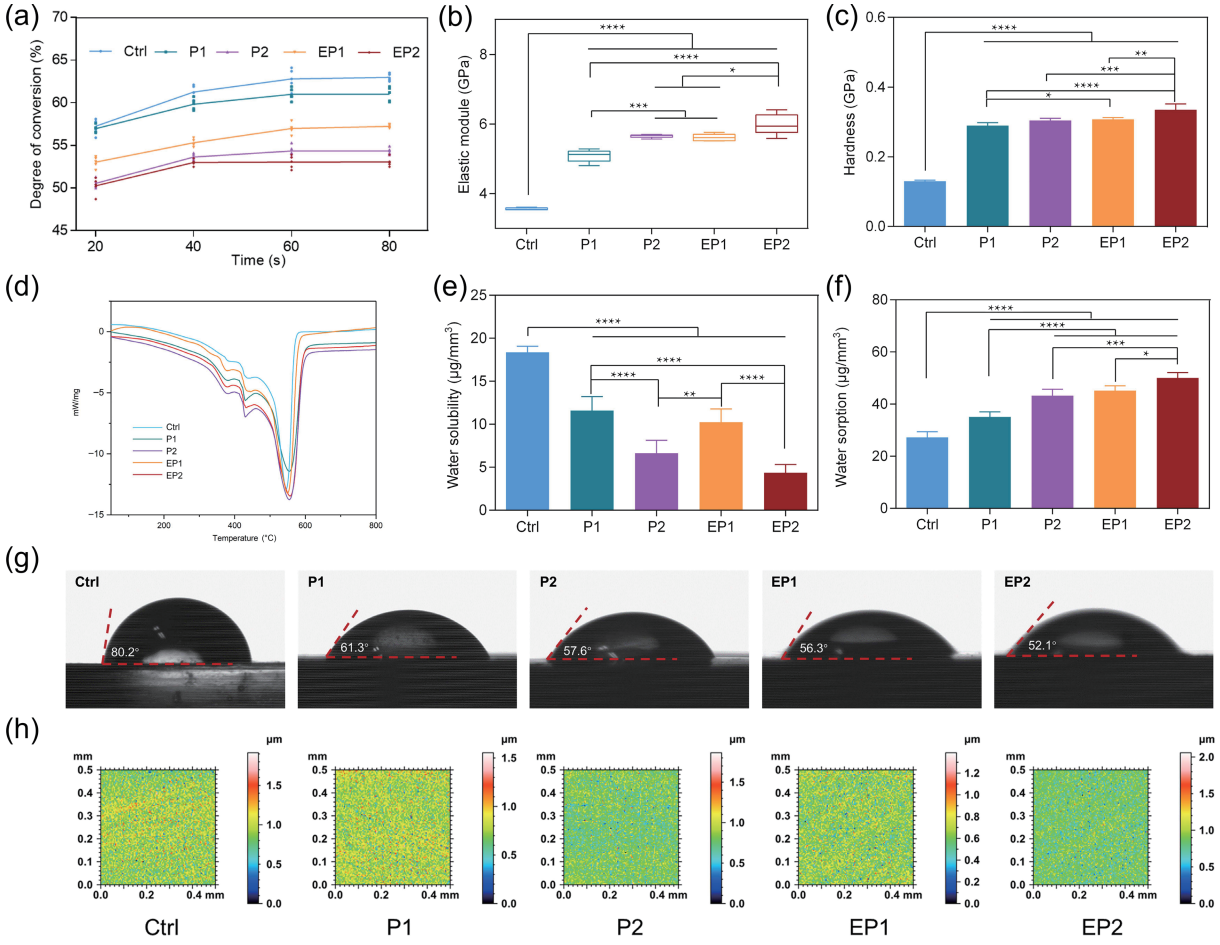

Figure 2 Physicochemical properties of TiO_2-ARCs. (a) Time-dependent degree of conversion of adhesive resins. (b) Elastic module, (c) surface hardness, (d) DSC curves, (e) water solubility, (f) water absorption, (g) water contact angles, and (h) two-dimensional optical profile of roughness of adhesive resins. Ctrl is blank control, and P1 and P2 are positive control with TiO_2 NPs. EP1 and EP2 are TiO_2-ARCs modified with TiO_2 NSs (mean ± SD; $^*p < 0.05$, $^{**}p < 0.01$, $^{***}p < 0.001$, and $^{****}p < 0.0001$).

between adhesion receptor on cell membrane and adhesion ligands on material surfaces. When surface exhibits moderate hydrophilicity, adhesion related molecules and proteins are more easily recognized by receptors and activate the adhesion motifs [52]. Also, higher elastic module and hardness can up-regulate cell adhesion. Cells in adhesion processes can generate tractional forces with substrate surface. Surface with harder elastic module and hardness can resist the tractional forces and the bio-active structure such as protein will not detach and promote cell adhesion [52]. Our results are consistent with the previous reports that cell adhesion and proliferation can be improved when the surface exhibits moderate hydrophilicity and harder rigidity [52, 53].

Furthermore, the application strategy is another regulator. Different with our results, some reports have demonstrated that TiO_2 nanostructures have adverse effect on cell bioactivity fate [54–56]. They suggested that TiO_2 nanostructures might express cytotoxicity because they produce reactive oxygen species (ROS). Also, when TiO_2 nanostructure was absorbed on cell lipid bilayer, it might change the membrane permeability and lead to cell death. Herein, the *in vitro* results illustrated that TiO_2 nanostructures presented no toxicity, also demonstrated bioactivity when they were used as fillers.

3.3.2 *Cell differentiation*

Considering the natural bio-effect of hDPSCs and the potential clinical application of resin materials in dentistry, we evaluated the osteogenic/odontogenic differentiation capacity of hDPSCs *in vitro*. The introduction of nano-TiO_2 can generate more alkaline phosphatase (ALP) and mineralize nodules at cell–resin interfaces (Figs. 4(a)–4(d)). These phenomena suggest that TiO_2 nanostructures can accelerate the induction of hDPSCs differentiation to osteogenic/odontogenic lineages. Related protein expression was convinced by WB test. Cell–resin interface modified with TiO_2 NSs can more strongly induce hDPSCs to differentiate to osteogenic/odontogenic lineage (Figs. 4(e) and 4(f)). We used RT-qPCR to further evaluate the gene expression related to osteogenic/odontogenic differentiation (Fig. 4(g)). Results showed hDPSCs cultured on resin surface of EP2 group exhibited significant gene upregulations on the 14th day ($p < 0.05$). Also, the degree of gene expression exhibited nano-TiO_2 concentration-dependent property.

The improved differentiation is highly related to enhanced mechanical properties of resin surfaces, including elastic module and hardness. It has been reported that mechanical strength of substrates' surface can regulate cell fates [57, 58]. The increase of surface mechanical strength can transfer the differentiation lineage of stem cells from neurogenic or adipogenic to osteogenic differentiation [40]. Also, the stretching and unfolding of the actin fibers mean that hDPSCs can expose more binding domains for the differentiation-related proteins or signaling molecules, such as Yes-associated protein (YAP), TAZ, FAK, and MAPK [59, 60]. These molecular sensors can regulate osteogenic/odontogenic differentiation through Hippo, ERK 1/2, and JNK MAPK pathways [59, 61]. Meanwhile, the increase of hDPSCs proliferation provides more candidates for differentiation and

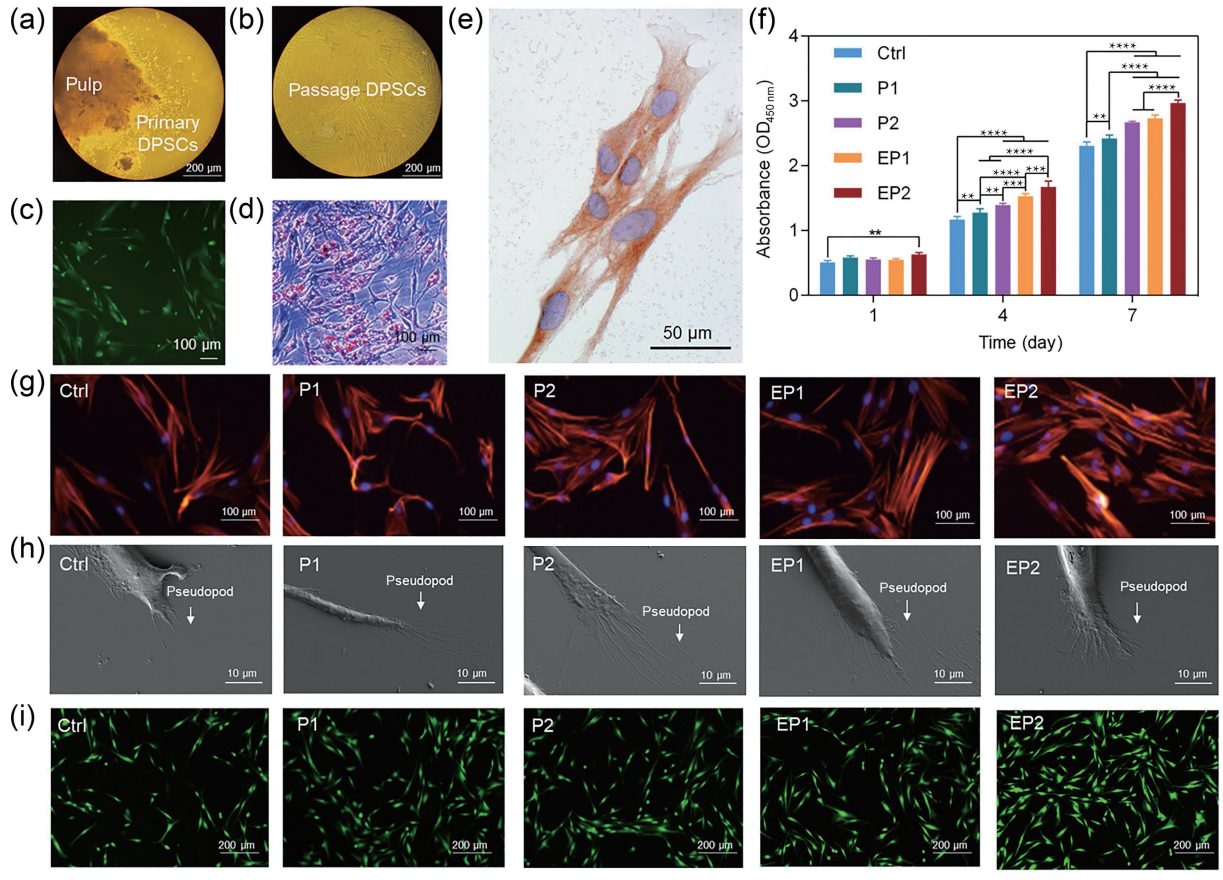

Figure 3 Regulation capacity of TiO_2-ARCs to adhesion and proliferation of hDPSCs. (a) The primary culture of hDPSCs. (b) The subculture culture of hDPSCs. (c) Immunofluorescence staining of NF-H. (d) Adipogenic differentiation of hDPSCs. (e) Immunohistochemical staining of STRO-1. (f) Proliferation of hDPSCs cultured on different resin discs by CCK-8. (g) Cytoskeleton staining of hDPSCs. (h) SEM observation of hDPSCs. (i) Cell viability of hDPSCs (mean ± SD; $^{**}p < 0.01$, $^{***}p < 0.001$, and $^{****}p < 0.0001$).

makes more osteogenic/odontogenic genes and protein expressions in the unit space of resin surfaces. While, considering the potential application in clinic, further *in vivo* researches are needed to verify the bio-effect of TiO_2 NSs on MTI.

3.4 Regulation capacity of TiO_2-ARCs to human dentin–resin hybrid interface

To explore the effect of nanomaterial dimension on MTI stability in multiple bionic environments, we designed a dentin–resin interface model based on micro-mechanical interlocking theory [62]. Exogenous ARCs prepared as described earlier were used to construct the nano–bio interface. Nano demineralized dentin collagen framework was prepared by acid etching. Then, nano-resin penetrates into the demineralized collagen network to form hybrid layer and resin tags (RT) to physically contact with collagen fibrils. After photo-curing procedure, resin components transfer from liquid to solid, graft, and wrap onto collagen fibrils. The resin nanocomposite fills the collagen network space to yield MTF (Fig. 5(a)).

Interface stability is manifested by the integrity of interface structures and bonding strengths. We firstly quantify the immediate micro-tensile strength to test whether the addition of TiO_2 nanostructure could adjust interface immediate mechanical behaviors. The results show that the micro-tensile strengths of all groups are similar ($p > 0.05$) (Figs. 5(b) and 5(c)). This indicates that TiO_2 nanostructure cannot change the interface immediate strengths. We further adopted matrix collagenase aging and thermocycling aging to mimic *in vivo* environments to explore the potential effect of TiO_2 nanostructure on interface stability (Fig. 5(d)). We find that all groups present lower micro-tensile strengths (Figs. 5(b) and 5(c), and Table S4 in the ESM). Strength of Ctrl separately dropped 52.4% and 49.4% after collagenase and thermocycling aging. While, with the introduction of TiO_2 nanostructure, the micro-tensile strength after aging increased. For example, EP2 exhibited the highest micro-tensile strength at 23.66 ± 2.31 MPa after collagenase aging and 27.35 ± 2.42 MPa after thermocycling, significantly higher than others ($p < 0.05$). Also, fracture mode analysis shows that the proportion of mixed fracture (with resin-dentin hybrid layer) decreases with the introduction of TiO_2 nanostructure at all conditions (Fig. 5(e) and Fig. S4 in the ESM), further indicating that NSs can improve the interface stability.

Compared to the control group, thicker hybrid interface forms after modifying adhesive resin with TiO_2 nanostructure (Fig. 5(f)). This means that the resin matrix modified with TiO_2 nanostructures has more bind sites with demineralized dentinal collagen which can increase the interface stability. Meanwhile, we used 50 wt.% ammoniacal silver nitrate solution [$Ag(NH_3)_2NO_3(aq)$] to evaluate the structural integrity of interface [63]. The silver ions can penetrate into the defect sites of interface. Figure 5(g) shows the silver deposition of EP2 is the lowest compared to other groups, suggesting that EP2 shows the best integrity of nano–bio interface.

Enhanced hydrophilicity of resin matrix is also considered as one important reason to improve resin–demineralized dentin collagen interaction. Collagen surface is composed with abundant hydrophilic groups such as –OH and $–NH_2$ [64]. Hence, the improvement of wettability means resin can more fully interact with demineralized collagen and wrap more collagen fibrils to increase micro-interlocking strength. Secondly, with the improvement of resin elastic module, average elastic module of

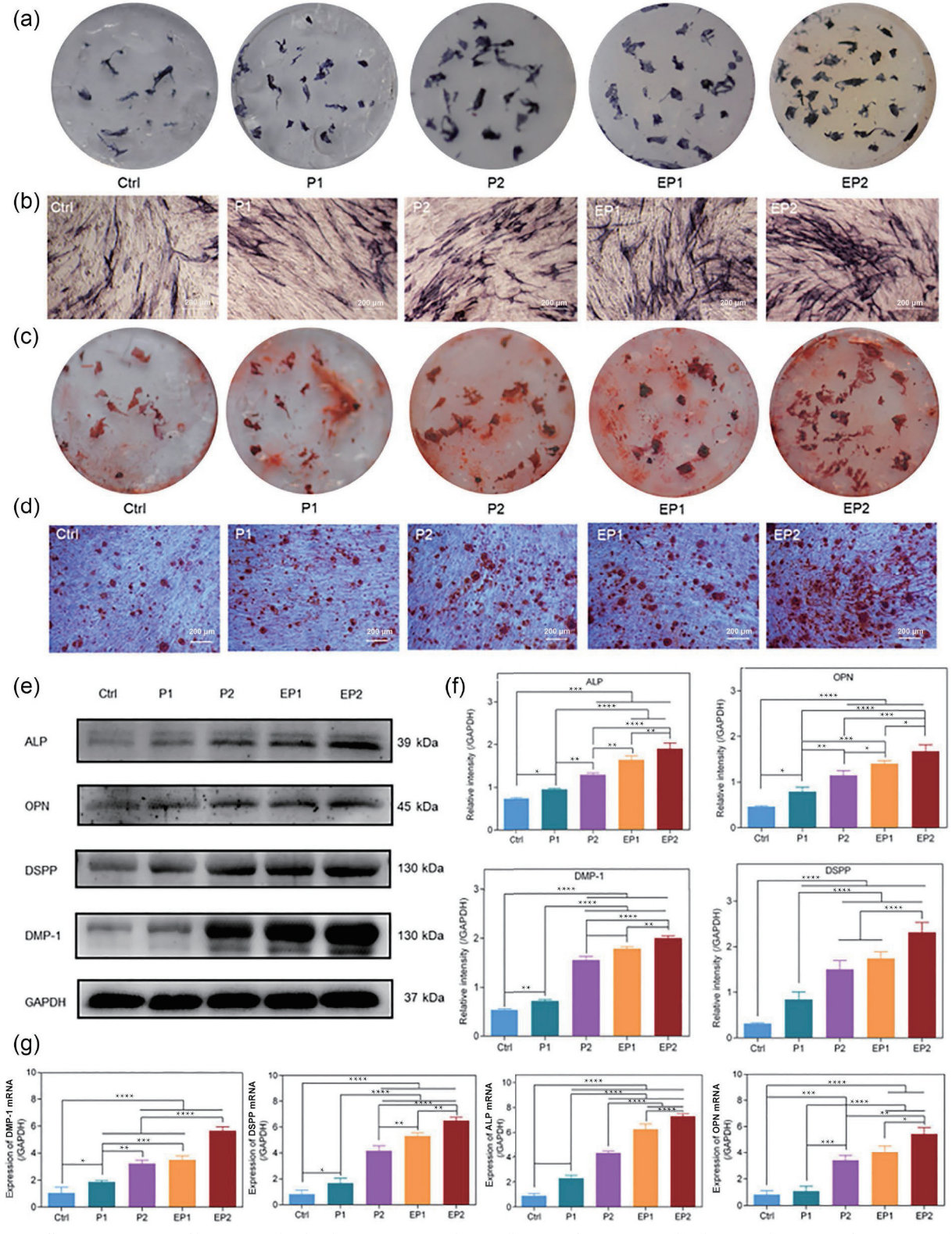

Figure 4 Differentiation capacity of hDPSCs regulated with TiO_2-ARCs. (a) The overall images of ALP staining. (b) The zoomed-in images of ALP staining. (c) The overall images of Alizarin red staining. (d) The zoomed-in images of Alizarin red staining. (e) WB of osteogenic/odontogenic-related proteins on the 14th day. (f) Quantitative assay of ALP, OPN, DMP-1, and DSPP protein expression on the 14th day. (g) Quantitative assay of osteogenic/odontogenic-related mRNA expression on the 14th day (mean ± SD; $^{*}p < 0.05$, $^{**}p < 0.01$, $^{***}p < 0.001$, and $^{****}p < 0.0001$).

resin-dentin hybrid layer can improve. We have found that the enhanced elastic module of hybrid layer is benefit for interface stability [65].

Roughness can also regulate the interaction between collagen fibers and resins. With the increase of roughness, the micro-interlocking strength can be enhanced. However, it is also benefit for the adhesion of bacteria that can dissociate the collagen three-helix structure, making the interface degradation [38]. Hence, the homeostasis of roughness after TiO_2 incorporation can also control the bacterial adhesion and has no adversely influence on the interface stability.

Worthwhile, it is still a contradiction whether the addition of nano materials could enhance the nano–bio interface stability. The incompatibility between nano materials and matrix may lead to

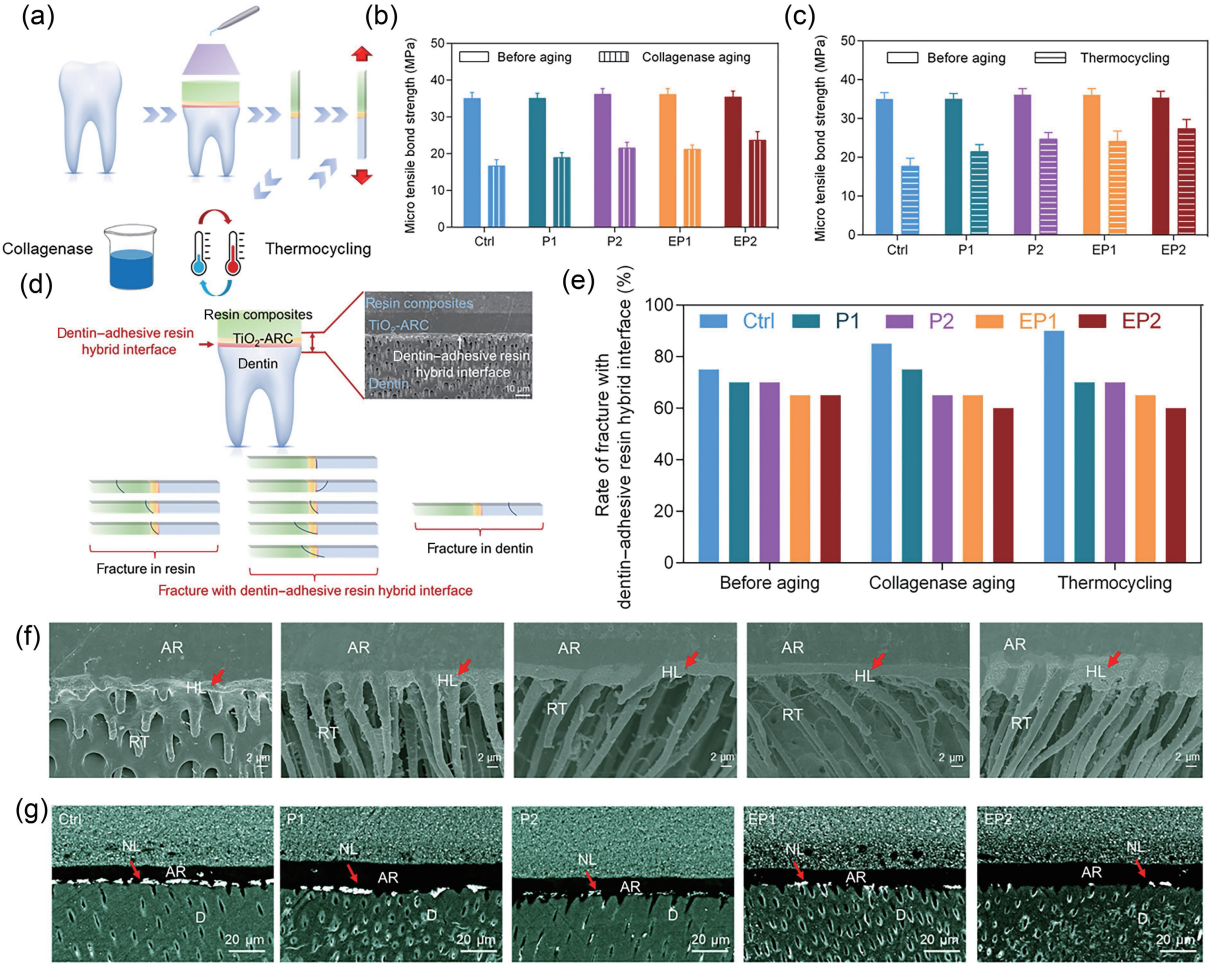

Figure 5 The effect of TiO_2-ARCs on dentin–resin hybrid interface stability. (a) Schematic diagram of construction of human dentin–resin hybrid interface. (b) Interface stability before and after collagenase aging. (c) Interface stability before and after thermocycling aging. (d) Schematic diagram of fracture mode. (e) Rate of fracture with dentin-adhesive resin hybrid interface before and after aging. (f) SEM of human dentin-adhesive resin hybrid interface (HL: dentin-adhesive resin hybrid interface). (g) Nanoleakage of dentin-adhesive resin hybrid interface (NL: nanoleakage at the bottom of hybrid interface; and D: dentin).

the existence of stress point and result in the uneven delivery of mechanical wave, while others demonstrate that the addition of void filler is significant for resin–dentin collagen bonding stability [66]. Our results are consistent with the latter. This suggests that TiO_2 NSs are useful to improve material–collagen interface and the results can be regarded as circumstantial evidence to prove the resin surface modified with TiO_2 NSs are homogeneous. The introduction of TiO_2 NSs can build stronger and more stable tissue-substrate hybrid layer.

4 Conclusions

In summary, we have demonstrated that the biomedical performances of polymer matrix composites can be effectively enhanced through tuning material–tissue interactions with TiO_2 NSs in sub-nanoscale. The key lies in exploring nanostructures that optimize the multiscale interfacial properties, including organic–inorganic hybridization interface, material–cell interface, and material–collagen interface. Our results show that atomically thin TiO_2 NSs are promising void fillers to improve the mechanical strength, hydrophilicity, stability, of resin matrixes. The material in sub-nanoscale can up-regulate the bioactivity of resin surface, provide a platform for hDPSCs adhesion, proliferation, and differentiation, and improve the interactions between resin matrix and dentinal collagen. This kind of nanocomposites has potential to improve the biological effect and interaction stability with bio-tissue of tissue engineering materials and drug delivery.

Acknowledgements

This work was supported by the National Natural Science Foundation of China (Nos. 82001110, 82071154, 21801012, 81720108011, 81470773, and 81571013).

Electronic Supplementary Material: Supplementary material (further details of fabrication and characterization of TiO_2 NSs and TiO_2-ARCs, the bioactivity evaluation of TiO_2-ARCs on hDPSCs, and the measurement of interaction with demineralized dentin collagen) is available in the online version of this article at https://doi.org/10.1007/s12274-022-5153-1.

References

[1] Zhang, H.; Zhang, Z. H.; Zhang, H.; Chen, C. W.; Zhang, D. G.; Zhao, Y. J. Protein-based hybrid responsive microparticles for wound healing. *ACS Appl. Mater. Interfaces* **2021**, *13*, 18413–18422.

[2] Wang, Y. A.; Zhang, J. W.; Zhao, Y.; Pu, M. J.; Song, X. Y.; Yu, L. M.; Yan, X. F.; Wu, J.; He, Z. Y. Innovations and challenges of polyphenol-based smart drug delivery systems. *Nano Res.* **2022**, *15*, 8156–8184.

[3] Kasper, M.; Ellenbogen, B.; Hardy, R.; Cydis, M.; Mojica-Santiago, J.; Afridi, A.; Spearman, B. S.; Singh, I.; Kuliasha, C. A.; Atkinson, E. et al. Development of a magnetically aligned regenerative tissue-engineered electronic nerve interface for peripheral nerve applications. *Biomaterials* **2021**, *279*, 121212.

[4] Nishimura, T.; Sasaki, Y.; Akiyoshi, K. Biotransporting self-assembled nanofactories using polymer vesicles with molecular

permeability for enzyme prodrug cancer therapy. *Adv. Mater.* **2017**, *29*, 1702406.
[5] Van Landuyt, K. L.; Snauwaert, J.; De Munck, J.; Peumans, M.; Yoshida, Y.; Poitevin, A.; Coutinho, E.; Suzuki, K.; Lambrechts, P.; Van Meerbeek, B. Systematic review of the chemical composition of contemporary dental adhesives. *Biomaterials* **2007**, *28*, 3757–3785.
[6] de Paula Rodrigues, M.; Soares, P. B. F.; Gomes, M. A. B.; Pereira, R. A.; Tantbirojn, D.; Versluis, A.; Soares, C. J. Direct resin composite restoration of endodontically-treated permanent molars in adolescents: Bite force and patient-specific finite element analysis. *J. Appl. Oral. Sci.* **2020**, *28*, e20190544.
[7] Maleckis, K.; Kamenskiy, A.; Lichter, E. Z.; Oberley-Deegan, R.; Dzenis, Y.; MacTaggart, J. Mechanically tuned vascular graft demonstrates rapid endothelialization and integration into the porcine iliac artery wall. *Acta Biomater.* **2021**, *125*, 126–137.
[8] Groen, W. M.; Diloksumpan, P.; Van Weeren, P. R.; Levato, R.; Malda, J. From intricate to integrated: Biofabrication of articulating joints. *J. Orthop. Res.* **2017**, *35*, 2089–2097.
[9] Gong, H. Y.; Hajizadeh, S.; Liu, W. F.; Ye, L. Imprinted polymer beads loaded with silver nanoparticles for antibacterial applications. *ACS Appl. Bio Mater.* **2021**, *4*, 2829–2838.
[10] Zheng, C.; Zhang, X. L.; Liu, W.; Liu, B.; Yang, H. H.; Lin, Z. A.; Chen, G. N. A selective artificial enzyme inhibitor based on nanoparticle–enzyme interactions and molecular imprinting. *Adv. Mater.* **2013**, *25*, 5922–5927.
[11] Liu, T. Y.; Li, L.; Cheng, C.; He, B. F.; Jiang, T. Y. Emerging prospects of protein/peptide-based nanoassemblies for drug delivery and vaccine development. *Nano Res.* **2022**, *15*, 7267–7285.
[12] Park, G.; Kim, H. O.; Lim, J. W.; Park, C.; Yeom, M.; Song, D.; Haam, S. Rapid detection of influenza A (H1N1) virus by conductive polymer-based nanoparticle via optical response to virus-specific binding. *Nano Res.* **2022**, *15*, 2254–2262.
[13] Tian, X. J.; Wang, Y.; Duan, S. M.; Hao, Y. J.; Zhao, K. X.; Li, Y.; Dai, R. T.; Wang, W. H. Evaluation of a novel nano-size collagenous matrix film cross-linked with gallotannins catalyzed by laccase. *Food Chem.* **2021**, *351*, 129335.
[14] Dhand, A. P.; Galarraga, J. H.; Burdick, J. A. Enhancing biopolymer hydrogel functionality through interpenetrating networks. *Trends Biotechnol.* **2021**, *39*, 519–538.
[15] Martin, J. R.; Howard, M. T.; Wang, S.; Berger, A. G.; Hammond, P. T. Oxidation-responsive, tunable growth factor delivery from polyelectrolyte-coated implants. *Adv. Healthc. Mater.* **2021**, *10*, 2001941.
[16] Gu, L. S.; Shan, T. T.; Ma, Y. X.; Tay, F. R.; Niu, L. N. Novel biomedical applications of crosslinked collagen. *Trends Biotechnol.* **2019**, *37*, 464–491.
[17] He, Q. L.; Liao, Y. G.; Zhang, J. W.; Yao, X. D.; Zhou, W. Y.; Hong, Y.; Ouyang, H. W. "All-in-one" gel system for whole procedure of stem-cell amplification and tissue engineering. *Small* **2020**, *16*, 1906539.
[18] Tian, K.; Suo, Z. G.; Vlassak, J. J. Chemically coupled interfacial adhesion in multimaterial printing of hydrogels and elastomers. *ACS Appl. Mater. Interfaces* **2020**, *12*, 31002–31009.
[19] Pinnaratip, R.; Bhuiyan, M. S. A.; Meyers, K.; Rajachar, R. M.; Lee, B. P. Multifunctional biomedical adhesives. *Adv. Healthc. Mater.* **2019**, *8*, 1801568.
[20] Zhou, J.; Gao, Z.; Xiang, G. L.; Zhai, T. Y.; Liu, Z. K.; Zhao, W. X.; Liang, X.; Wang, L. Y. Interfacial compatibility critically controls Ru/TiO_2 metal–support interaction modes in CO_2 hydrogenation. *Nat. Commun.* **2022**, *13*, 327.
[21] Tang, X. M.; Huang, K.; Dai, J.; Wu, Z. Y.; Cai, L.; Yang, L. L.; Wei, J.; Sun, H. L. Influences of surface treatments with abrasive paper and sand-blasting on surface morphology, hydrophilicity, mineralization and osteoblasts behaviors of n-CS/PK composite. *Sci. Rep.* **2017**, *7*, 568.
[22] Cabrera, I. C.; Berlioz, S.; Fahs, A.; Louarn, G.; Carriere, P. Chemical functionalization of Nano fibrillated cellulose by glycidyl silane coupling agents: A grafted silane network characterization study. *Int. J. Biol. Macromol.* **2020**, *165*, 1773–1782.
[23] Xu, R. C.; Yu, F.; Huang, L.; Zhou, W.; Wang, Y.; Wang, F.; Sun, X.; Chang, G.; Fang, M.; Zhang, L. et al. Isocyanate-terminated urethane-based dental adhesive bridges dentinal matrix collagen with adhesive resin. *Acta Biomater.* **2019**, *83*, 140–152.
[24] Arno, M. C.; Inam, M.; Weems, A. C.; Li, Z. H.; Binch, A. L. A.; Platt, C. I.; Richardson, S. M.; Hoyland, J. A.; Dove, A. P.; O'Reilly, R. K. Exploiting the role of nanoparticle shape in enhancing hydrogel adhesive and mechanical properties. *Nat. Commun.* **2020**, *11*, 1420.
[25] Stojanović, Z. S.; Ignjatović, N.; Wu, V.; Žunič, V.; Veselinović, L.; Škapin, S.; Miljković, M.; Uskoković, V.; Uskoković, D. Hydrothermally processed 1D hydroxyapatite: Mechanism of formation and biocompatibility studies. *Mater. Sci. Eng. :C* **2016**, *68*, 746–757.
[26] Zhang, Y. G.; Li, J. P.; Mouser, V. H. M.; Roumans, N.; Moroni, L.; Habibovic, P. Biomimetic mechanically strong one-dimensional hydroxyapatite/poly(D, L-lactide) composite inducing formation of anisotropic collagen matrix. *ACS Nano* **2021**, *15*, 17480–17498.
[27] Zhang, J. Y.; Chen, H. L.; Zhao, M.; Liu, G. T.; Wu, J. 2D nanomaterials for tissue engineering application. *Nano Res.* **2020**, *13*, 2019–2034.
[28] Azizi-Lalabadi, M.; Jafari, S. M. Bio-nanocomposites of graphene with biopolymers; fabrication, properties, and applications. *Adv. Colloid Interface Sci.* **2021**, *292*, 102416.
[29] Qu, G. B.; Xia, T.; Zhou, W. H.; Zhang, X.; Zhang, H. Y.; Hu, L. G.; Shi, J. B.; Yu, X. F.; Jiang, G. B. Property–activity relationship of black phosphorus at the nano–bio interface: From molecules to organisms. *Chem. Rev.* **2020**, *120*, 2288–2346.
[30] Chuang, Y. C.; Chang, C. C.; Yang, F.; Simon, M.; Rafailovich, M. TiO_2 nanoparticles synergize with substrate mechanics to improve dental pulp stem cells proliferation and differentiation. *Mater. Sci. Eng. :C* **2021**, *118*, 111366.
[31] Kantovitz, K. R.; Fernandes, F. P.; Feitosa, I. V.; Lazzarini, M. O.; Denucci, G. C.; Gomes, O. P.; Giovani, P. A.; Moreira, K. M. S.; Pecorari, V. G. A.; Borges, A. F. S. et al. TiO_2 nanotubes improve physico-mechanical properties of glass ionomer cement. *Dent. Mater.* **2020**, *36*, e85–e92.
[32] Wang, M. H.; Wang, Q.; Wang, K. F.; Lu, X. Functionalized TiO_2 surfaces facilitate selective receptor-recognition and modulate biological function of bone morphogenetic protein-2. *J. Phys. Chem. C* **2018**, *122*, 29319–29329.
[33] Xiang, G. L.; Tang, Y.; Liu, Z. G.; Zhu, W.; Liu, H. T.; Wang, J. O.; Zhong, G. M.; Li, J.; Wang, X. Probing ligand-induced cooperative orbital redistribution that dominates nanoscale molecule–surface interactions with one-unit-thin TiO_2 nanosheets. *Nano Lett.* **2018**, *18*, 7809–7815.
[34] Xiang, G. L.; Wang, Y. G. Exploring electronic-level principles how size reduction enhances nanomaterial surface reactivity through experimental probing and mathematical modeling. *Nano Res.* **2022**, *15*, 3812–3817.
[35] Ma, S. Q.; Zhao, W. X.; Zhou, J.; Wang, J. O.; Chu, S. Q.; Liu, Z. G.; Xiang, G. L. A new type of noncovalent surface–π stacking interaction occurring on peroxide-modified titania nanosheets driven by vertical π-state polarization. *Chem. Sci.* **2021**, *12*, 4411–4417.
[36] Yamauchi, S.; Wang, X.; Egusa, H.; Sun, J. High-performance dental adhesives containing an ether-based monomer. *J. Dent. Res.* **2020**, *99*, 189–195.
[37] Bendary, I. M.; Garcia, I. M.; Collares, F. M.; Takimi, A.; Samuel, S. M. W.; Leitune, V. C. B. Wollastonite as filler of an experimental dental adhesive. *J. Dent.* **2020**, *102*, 103472.
[38] Montoya, C.; Jain, A.; Londoño, J. J.; Correa, S.; Lelkes, P. I.; Melo, M. A.; Orrego, S. Multifunctional dental composite with piezoelectric nanofillers for combined antibacterial and mineralization effects. *ACS Appl. Mater. Interfaces* **2021**, *13*, 43868–43879.
[39] Cadenaro, M.; Maravic, T.; Comba, A.; Mazzoni, A.; Fanfoni, L.; Hilton, T.; Ferracane, J.; Breschi, L. The role of polymerization in adhesive dentistry. *Dent Mater.* **2019**, *35*, e1–e22.
[40] Ye, K.; Wang, X.; Cao, L. P.; Li, S. Y.; Li, Z. H.; Yu, L.; Ding, J. D. Matrix stiffness and nanoscale spatial organization of cell-adhesive ligands direct stem cell fate. *Nano Lett.* **2015**, *15*, 4720–4729.

[41] Martos, R.; Hegedüs, V.; Szalóki, M.; Blum, I. R.; Lynch, C. D.; Hegedüs, C. A randomised controlled study on the effects of different surface treatments and adhesive self-etch functional monomers on the immediate repair bond strength and integrity of the repaired resin composite interface. *J. Dent.* **2019**, *85*, 57–63.

[42] Yao, C. M.; Ahmed, M. H.; Li, X.; Nedeljkovic, I.; Vandooren, J.; Mercelis, B.; Zhang, F.; Van Landuyt, K. L.; Huang, C.; Van Meerbeek, B. Zinc-calcium-fluoride bioglass-based innovative multifunctional dental adhesive with thick adhesive resin film thickness. *ACS Appl. Mater. Interfaces* **2020**, *12*, 30120–30135.

[43] Yu, F.; Xu, R. C.; Huang, L.; Luo, M. L.; Li, J.; Tay, F. R.; Niu, L. N.; Chen, J. H. Isocyanate-terminated urethane-based methacrylate for *in situ* collagen scaffold modification. *Mater. Sci. Eng. :C* **2020**, *112*, 110902.

[44] Chen, K.; Tang, X. K.; Jia, B. B.; Chao, C. Z.; Wei, Y.; Hou, J. Y.; Dong, L. T.; Deng, X. L.; Xiao, T. H.; Goda, K. et al. Graphene oxide bulk material reinforced by heterophase platelets with multiscale interface crosslinking. *Nat. Mater.* **2022**, *21*, 1121–1129.

[45] Hosseinpour, S.; Tang, F. J.; Wang, F. L.; Livingstone, R. A.; Schlegel, S. J.; Ohto, T.; Bonn, M.; Nagata, Y.; Backus, E. H. G. Chemisorbed and physisorbed water at the TiO_2/water interface. *J. Phys. Chem. Lett.* **2017**, *8*, 2195–2199.

[46] Yoshimitsu, Z.; Nakajima, A.; Watanabe, T.; Hashimoto, K. Effects of surface structure on the hydrophobicity and sliding behavior of water droplets. *Langmuir* **2002**, *18*, 5818–5822.

[47] Shakir, M.; Jolly, R.; Khan, A. A.; Ahmed, S. S.; Alam, S.; Rauf, M. A.; Owais, M.; Farooqi, M. A. Resol based chitosan/nano-hydroxyapatite nanoensemble for effective bone tissue engineering. *Carbohydr. Polym.* **2018**, *179*, 317–327.

[48] Chen, L.; Suh, B. I. Cytotoxicity and biocompatibility of resin-free and resin-modified direct pulp capping materials: A state-of-the-art review. *Dent. Mater. J.* **2017**, *36*, 1–7.

[49] Garcia, I. M.; Balhaddad, A. A.; Lan, Y. C.; Simionato, A.; Ibrahim, M. S.; Weir, M. D.; Masri, R.; Xu, H. H. K.; Collares, F. M.; Melo, M. A. S. Magnetic motion of superparamagnetic iron oxide nanoparticles-loaded dental adhesives: Physicochemical/biological properties, and dentin bonding performance studied through the tooth pulpal pressure model. *Acta Biomater.* **2021**, *134*, 337–347.

[50] Di Cio, S.; Gautrot, J. E. Cell sensing of physical properties at the nanoscale: Mechanisms and control of cell adhesion and phenotype. *Acta Biomater.* **2016**, *30*, 26–48.

[51] Cui, Y. D.; Hameed, F. M.; Yang, B.; Lee, K.; Pan, C. Q.; Park, S.; Sheetz, M. Cyclic stretching of soft substrates induces spreading and growth. *Nat. Commun.* **2015**, *6*, 6333.

[52] Bacakova, L.; Filova, E.; Parizek, M.; Ruml, T.; Svorcik, V. Modulation of cell adhesion, proliferation and differentiation on materials designed for body implants. *Biotechnol. Adv.* **2011**, *29*, 739–767.

[53] Martins, J. G.; Camargo, S. E. A.; Bishop, T. T.; Popat, K. C.; Kipper, M. J.; Martins, A. F. Pectin-chitosan membrane scaffold imparts controlled stem cell adhesion and proliferation. *Carbohydr. Polym.* **2018**, *197*, 47–56.

[54] Lee, W. A.; Pernodet, N.; Li, B. Q.; Lin, C. H.; Hatchwell, E.; Rafailovich, M. H. Multicomponent polymer coating to block photocatalytic activity of TiO_2 nanoparticles. *Chem. Commun.* **2007**, 4815–4817.

[55] Vevers, W. F.; Jha, A. N. Genotoxic and cytotoxic potential of titanium dioxide (TiO_2) nanoparticles on fish cells *in vitro*. *Ecotoxicology* **2008**, *17*, 410–420.

[56] Park, E. J.; Yi, J.; Chung, K. H.; Ryu, D. Y.; Choi, J.; Park, K. Oxidative stress and apoptosis induced by titanium dioxide nanoparticles in cultured BEAS-2B cells. *Toxicol. Lett.* **2008**, *180*, 222–229.

[57] Feng, Q.; Gao, H. C.; Wen, H. J.; Huang, H. H.; Li, Q. T.; Liang, M. H.; Liu, Y.; Dong, H. Cao, X. D. Engineering the cellular mechanical microenvironment to regulate stem cell chondrogenesis:Insights from a microgel model. *Acta Biomater.* **2020**, *113*, 393–406.

[58] Liu, Y. H.; Zhu, Z.; Pei, X. B.; Zhang, X.; Cheng, X. T.; Hu, S. S.; Gao, X. M.; Wang, J.; Chen, J. Y.; Wan, Q. B. ZIF-8-modified multifunctional bone-adhesive hydrogels promoting angiogenesis and osteogenesis for bone regeneration. *ACS Appl. Mater. Interfaces* **2020**, *12*, 36978–36995.

[59] Li, J.; Yan, J. F.; Wan, Q. Q.; Shen, M. J.; Ma, Y. X.; Gu, J. T.; Gao, P.; Tang, X. Y.; Yu, F.; Chen, J. H. et al. Matrix stiffening by self-mineralizable guided bone regeneration. *Acta Biomater.* **2021**, *125*, 112–125.

[60] Majidinia, M.; Sadeghpour, A.; Yousefi, B. The roles of signaling pathways in bone repair and regeneration. *J. Cell. Physiol.* **2018**, *233*, 2937–2948.

[61] Yu, W. Q.; Qian, C.; Jiang, X. Q.; Zhang, F. Q.; Weng, W. M. Mechanisms of stem cell osteogenic differentiation on TiO_2 nanotubes. *Colloids Surf. B: Biointerfaces* **2015**, *136*, 779–785.

[62] De Munck, J.; Van Landuyt, K.; Peumans, M.; Poitevin, A.; Lambrechts, P.; Braem, M.; Van Meerbeek, B. A critical review of the durability of adhesion to tooth tissue: Methods and results. *J. Dent. Res.* **2005**, *84*, 118–132.

[63] Freitas, P. H.; André, C. B.; Fronza, B. M.; Giannini, M.; Rosalen, P. L.; Consani, S.; França, R. Physicochemical properties, metalloproteinases inhibition, and antibiofilm activity of doxycycline-doped dental adhesive. *J. Dent.* **2021**, *104*, 103550.

[64] Shoulders, M. D.; Raines, R. T. Collagen structure and stability. *Annu. Rev. Biochem.* **2009**, *78*, 929–958.

[65] Yu, F.; Luo, M. L.; Xu, R. C.; Huang, L.; Yu, H. H.; Meng, M.; Jia, J. Q.; Hu, Z. H.; Wu, W. Z.; Tay, F. R. et al. A novel dentin bonding scheme based on extrafibrillar demineralization combined with covalent adhesion using a dry-bonding technique. *Bioact. Mater.* **2021**, *6*, 3557–3567.

[66] Cai, X.; Wang, X. Y. Chlorhexidine-loaded poly(amido amine) dendrimer and a dental adhesive containing amorphous calcium phosphate nanofillers for enhancing bonding durability. *Dent. Mater.* **2022**, *38*, 824–834.